



Rapid analysis of metal ions and organic compounds in strong acidic solutions by nano-ESI mass spectrometry

Jiaquan Xu^a, Ting Li^a, Zhendong Yu^a, Lili Song^a, Xiu-Xiu Xu^{b,*}, Hui Li^{a,*}

^a Jiangxi Key Laboratory for Mass Spectrometry and Instrumentation, East China University of Technology, Nanchang 330013, China

^b Department of Rehabilitation Medicine, The First Affiliated Hospital of Nanchang University, Nanchang 330006, China

ARTICLE INFO

Article history:

Received 22 November 2022

Revised 24 April 2023

Accepted 14 May 2023

Available online 20 May 2023

Keywords:

Strong acidic solutions

Nano-ESI MS

Rapid analysis

Reaction monitoring

Micro-area analysis

Gastric juice analysis

ABSTRACT

Rapid analysis of metal ions and organic compounds in strong acidic solutions is of sustainable interest in multiple disciplines. However, complicated and time-consuming pretreatments are always required for MS analysis of the compounds in strong acidic solutions. Otherwise, it will result in a weak signal and cause serious damage to the mass spectrometer. Herein, a simple method inherited from nano-ESI MS was developed for rapid analysis of strong acidic solutions. Nanoliter (nL) strong acidic solution was first loaded in the nano-ESI emitter, followed by evaporation to remove the H⁺ and leave the analytes on the wall of the nano-ESI emitter. The evaporation process can be completed within 1 min because of the extremely tiny volume (≤ 1 nL) of the loaded solution. Then, the dried analytes on the wall of the nano-ESI emitter were redissolved by loading a new solvent, followed by nano-ESI MS analysis. By using this method, metal ions and organic compounds in the strong acidic solution can be detected with low sample consumption (1 nL), high speed (< 2 min/sample), high sensitivity (limit of detection = 0.2 $\mu\text{g/L}$), and high accuracy ($> 90\%$). Proof-of-concept applications of the present method have been successfully achieved for the analysis of gastric juice (pH of the sample = 1), monitoring reaction catalyzed by strong acid (pH of the system = 0), and micro-area analysis of ores (pH of the extraction solvent = 0), showing great application potential in multiple fields.

© 2023 Published by Elsevier B.V. on behalf of Chinese Chemical Society and Institute of Materia Medica, Chinese Academy of Medical Sciences.

The strong acidic solutions are ubiquitous samples available in various fields, including gastric juice in life sciences [1], strong acidic wastewater in the environment field [2], strong acidic extracting solutions of ores in geology [3], strong acidic electrolytes used for electroplating or electropolishing in industry [4], strong acid catalytic reactions in chemical synthesis [5], acidic food [6], and so on. Rapid analysis of the compounds in these acidic solutions has great significance for understanding their physicochemical properties. For instance, the metabolites in gastric juice are useful for the diagnosis and treatment of diseases [7–10]. The information of compounds in acidic wastewater contributes to the safety assessment, pollutant traceability, and wastewater treatment [11]. The grade of ores can be determined by analysis of the extracting solutions of ores which are usually strong acidic solutions [12,13]. Monitoring the components in strong acidic catalytic reactions in real-time is useful for understanding the reaction processes and mechanisms [14]. Analysis of the trace impurities in

semiconductor-grade hydrochloric acids can be used for evaluation of the product qualities [15].

Mass spectrometry (MS) is a powerful analytical method with the advantages of high throughput, high sensitivity, and excellent performance for chemical structure identification. But at present, complex sample pretreatment is always required for MS analysis of the strong acidic solution, otherwise the strong acid with high concentration would damage the instrument and weaken the MS signal. For example, gastric juice often needs to be diluted 1000 times with normal saline prior to MS analysis [16–18], such as thermal desorption electrospray ionization/mass spectrometry (TD-ESI/MS) [19–21]. Wastewater has to be treated with dilution and extraction before analyzing by MS [22] or SPME/GC-MS [23]. On the other hand, evaporation was always carried out to remove the acid, followed by redissolution with the appropriate solution for instrumental analysis [24]. These complex sample pretreatments would cause a large consumption of sample, labor, and analytical time [25–27]. For example, it takes about 2–3 h to remove acid from ore extracts.

In this paper, a simple method was developed for rapid analysis of strong acidic solutions by nano electrospray ionization mass

* Corresponding authors.

E-mail addresses: xiuxiu-xu@foxmail.com (X.-X. Xu), huili_201860188@ecut.edu.cn (H. Li).

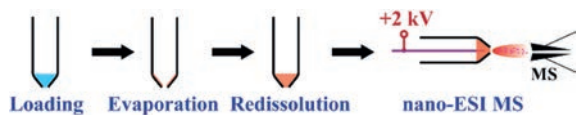


Fig. 1. Schematic diagram of the ER-nano-ESI MS for the analysis of strong acidic solution.

spectrometry (nano-ESI MS). As shown in Fig. 1, nanoliter strong acidic solution was first loaded in the nano-ESI emitter. Then, evaporation was used to remove the solvent and acid, and the analytes would be left on the wall of the nano-ESI emitter tip. After that, a new solvent was loaded in the nano-ESI emitter to redissolve the residual analytes for nano-ESI MS analysis. Because the analytical process consisted of “Evaporation”, “Redissolution” and “nano-ESI MS”, the present method was named “ER-nano-ESI MS”. This ER-nano-ESI MS method takes the advantages of high analytical speed, low sample consumption, and little labor consumption.

In advance of the experiments, the following materials were prepared. Platinum wire with diameter of 100 μm was purchased from the Junlilai company (Jiangsu, China). Quartz capillary (B100-75-10, 0.50 mm i.d., 1.00 mm o.d., Sutter Instrument Company, American) was used to prepare a micropipette with a defined tip size by a laser puller (P1000, Sutter Instrument Company, American). Ethylenediaminetetraacetic acid (EDTA), $\text{Cu}(\text{NO}_3)_2 \cdot 3\text{H}_2\text{O}$, phenanthroline (Phen), HNO_3 , and HCl were purchased from Sinopharm Chemical Reagent Co., Ltd. CH_3OH with chromatographic purity was purchased from Merck. The experimental ultrapure water was produced by the Barnstead Nanopure ultrapure water system (Thermo Fisher Scientific). All chemicals unless specified were reagent grade and were used as received. During the experiments, the following instruments were involved. A commercial mass spectrometer (LTQ-Orbitrap-MS, Thermo Fisher Scientific), equipped with Xcalibur 2.2 data processing system, was hired to carry out the analysis of compounds. Scanning electron microscopy (Oxford Instruments) was used to characterize the morphology of the nano-ESI emitter.

The experimental procedure is schematically shown in Fig. 1, which involved three critical steps “Evaporation”, “Redissolution” and “nano-ESI MS analysis”. Typically, nanoliter strong acidic solution was first sucked into the laser-pulled micropipette. The volume of the sucked sample solution can be precisely controlled by fixing the height of liquid (Fig. S1a in Supporting information) in the micropipette by a microinjector under a microscope. Secondly, the micropipette was hung above a heating plate with the tip downwards. The distance between the micropipette tip and the heating plate was 1 cm. The solution in the micropipette was evaporated accompanying with the removal of the acid and the analytes remained on the wall. This “Evaporation” process could be completed within 1 min because the volume of the loaded solution was extremely tiny. Subsequently, a fresh new solvent (e.g., $\text{CH}_3\text{OH}/\text{H}_2\text{O}$, $v/v = 1:1$) was loaded in the micropipette to dissolve the residual analytes with the assistance of ultrasonic. What calls for special attention is that the micropipette cannot be treated by ultrasonic directly in a solution because its tip is open and delicate. Thus, a glass rod was added to transmit vibration to the micropipette. During operation, the glass rod was placed against the bottom of the sonicator, and the micropipette was attached to the glass rod. This “Redissolution” process can be completed within 0.5 min. After that, the micropipette was used as a nano-ESI emitter to ionize the analytes at $+2\text{ kV}/-2\text{ kV}$ for MS analysis, which also can be completed within 0.5 min.

$\text{Cu}(\text{NO}_3)_2$ was first used to test the performance of ER-nano-ESI MS for analysis of the metal ion. According to our previous reports [28], metal ions can be detected in the form of metal-organic chelates in organic MS and the signal intensity has pos-

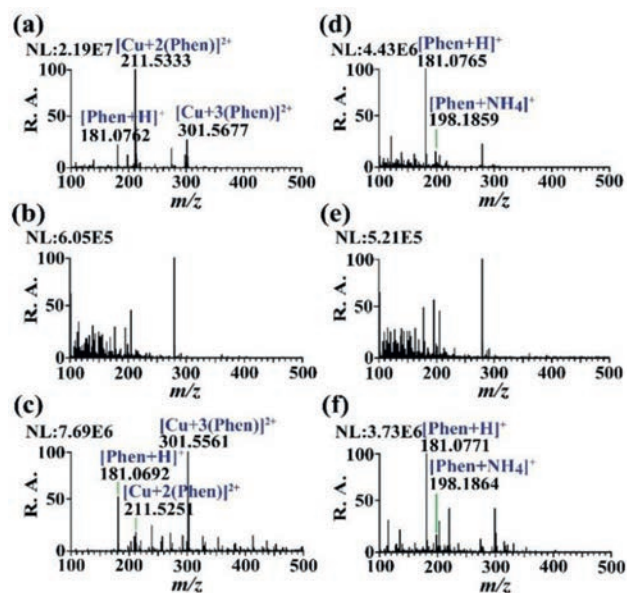


Fig. 2. Analysis of metal ions and organic compounds by nano-ESI MS and ER-nano-ESI MS. (a) Mass spectrum of 500 $\mu\text{g/L}$ Phen and 100 $\mu\text{g/L}$ $\text{Cu}(\text{NO}_3)_2$ in $\text{CH}_3\text{OH}/\text{H}_2\text{O}$ solution obtained by nano-ESI MS. (b) Mass spectrum of 500 $\mu\text{g/L}$ Phen and 100 $\mu\text{g/L}$ $\text{Cu}(\text{NO}_3)_2$ in 0.1 mol/L HNO_3 $\text{CH}_3\text{OH}/\text{H}_2\text{O}$ solution obtained by nano-ESI MS. (c) Mass spectrum of 500 $\mu\text{g/L}$ Phen and 100 $\mu\text{g/L}$ $\text{Cu}(\text{NO}_3)_2$ in 0.1 mol/L HNO_3 $\text{CH}_3\text{OH}/\text{H}_2\text{O}$ solution obtained by ER-nano-ESI MS. (d) Mass spectrum of 100 $\mu\text{g/L}$ Phen in $\text{CH}_3\text{OH}/\text{H}_2\text{O}$ solution obtained by nano-ESI MS. (e) Mass spectrum of 100 $\mu\text{g/L}$ Phen in 0.1 mol/L HNO_3 $\text{CH}_3\text{OH}/\text{H}_2\text{O}$ solution obtained by nano-ESI MS. (f) Mass spectrum of 100 $\mu\text{g/L}$ Phen in 0.1 mol/L HNO_3 $\text{CH}_3\text{OH}/\text{H}_2\text{O}$ solution obtained by ER-nano-ESI MS. R. A. is the abbreviation of relative abundance.

itive correlation with the stability constant of chelate. Phen is widely employed as the ligand for metal-organic chelate with high stability constant. As shown in Fig. 2a, obvious signals of $[\text{Phen} + \text{H}]^+$, $[\text{Cu} + 2(\text{Phen})]^{2+}$, and $[\text{Cu} + 3(\text{Phen})]^{2+}$ were obtained by nano-ESI MS when 1 μL of 500 mg/L Phen was added in 1 mL of 100 $\mu\text{g/L}$ $\text{Cu}(\text{NO}_3)_2$ $\text{CH}_3\text{OH}/\text{H}_2\text{O}$ ($v/v = 1/1$) solution. However, the three signals were almost invisible (Fig. 2b) when 1 μL of 500 $\mu\text{g/L}$ Phen was added in 1 mL of 100 $\mu\text{g/L}$ $\text{Cu}(\text{NO}_3)_2$ 0.1 mol/L HNO_3 $\text{CH}_3\text{OH}/\text{H}_2\text{O}$ ($v/v = 1:1$) solution, of which the pH was tested to be 1 by a pH test paper (Fig. S2a in Supporting information). One possible explanation was that the high concentration ion resulted from HNO_3 suppressed the spray which was observed during the experimental process. Besides, the pH can also affect the chelation between ligand and metal ion, which is closely related to the intensity of MS signal. In ER-nano-ESI MS, 1 nL of 100 $\mu\text{g/L}$ $\text{Cu}(\text{NO}_3)_2$ in 0.1 mol/L HNO_3 $\text{CH}_3\text{OH}/\text{H}_2\text{O}$ ($v/v = 1/1$) was first loaded in the micropipette, followed by evaporation at 100 $^\circ\text{C}$ (Fig. S3a in Supporting information) for 1 min to remove HNO_3 and leave $\text{Cu}(\text{NO}_3)_2$ on the wall of the micropipette. Note that, a higher evaporation temperature of 150 $^\circ\text{C}$ led to a weaker signal. The probable reason is that $\text{Cu}(\text{NO}_3)_2$ may be decomposed to CuO partly at 150 $^\circ\text{C}$, a temperature close to the thermolysis temperature of $\text{Cu}(\text{NO}_3)_2$ (175 $^\circ\text{C}$), and CuO is much more difficult to be dissolved by Phen than $\text{Cu}(\text{NO}_3)_2$. After that, 1 nL of 500 $\mu\text{g/L}$ Phen $\text{CH}_3\text{OH}/\text{H}_2\text{O}$ ($v/v = 1/1$) solution was loaded in the micropipette to dissolve and chelate the residual $\text{Cu}(\text{NO}_3)_2$ with the assistance of ultrasonic for 30 s (Fig. S3b in Supporting information). The pH of the solution was tested to be 6 (Fig. S2b in Supporting information), indicating that the acid was almost completely removed during the “Evaporation” procedure. Finally, the chelates were analyzed using the micropipette as a nano-ESI emitter. Consequently, obvious signals of $[\text{Cu} + 2(\text{Phen})]^{2+}$ (m/z 211.5333) and $[\text{Cu} + 3(\text{Phen})]^{2+}$ (m/z 301.5677) were observed (Fig. 2c) and the intensity was comparable to that in Fig. 2a with $>90\%$ recovery,

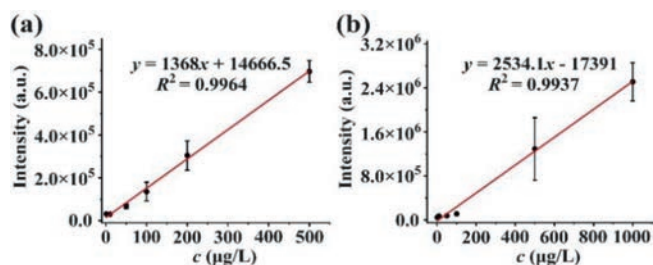


Fig. 3. The standard curves of intensities of the characteristic ions versus concentrations of the analytes. (a) Intensity of $[^{63}\text{Cu} + 2(\text{Phen})]^{2+} + [^{63}\text{Cu} + 3(\text{Phen})]^{2+}$ vs. concentration of Cu^{2+} . (b) Intensity of $[\text{Phen} + \text{H}]^+$ vs. concentration of Phen. The Cu^{2+} and Phen were all dissolved in 0.1 mol/L HNO_3 solutions and detected by ER-nano-ESI MS. The error bar represents the standard deviation of three replicates.

indicating that the residual $\text{Cu}(\text{NO}_3)_2$ was mostly dissolved during the “Redissolution” procedure. These results speak volumes for the effectiveness of ER-nano-ESI MS for analyzing metal ion in strong acidic solution with rapidness (<2 min/sample) and accuracy (>90%).

Likewise, Phen was used to investigate the performance of ER-nano-ESI MS for analysis of the organic analyte in strong acidic solution. Fig. 2d displayed the result of 100 μg/L Phen in $\text{CH}_3\text{OH}/\text{H}_2\text{O}$ ($v/v = 1/1$) obtained by nano-ESI MS, and a conspicuous signal of $[\text{Phen} + \text{H}]^+$ (m/z 181.0765) was observed. However, the peak of $[\text{Phen} + \text{H}]^+$ almost disappeared (Fig. 2e) when 100 μg/L Phen in 0.1 mol/L HNO_3 $\text{CH}_3\text{OH}/\text{H}_2\text{O}$ ($v/v = 1/1$) was analyzed by nano-ESI MS. In ER-nano-ESI MS, 1 nL of 100 μg/L Phen in 0.1 mol/L HNO_3 $\text{CH}_3\text{OH}/\text{H}_2\text{O}$ ($v/v = 1/1$) was first loaded in the micropipette, followed by evaporation at 150 °C (Fig. S3c in Supporting information) for 1 min to remove HNO_3 and leave Phen on the wall of the micropipette. Then, 1 nL $\text{CH}_3\text{OH}/\text{H}_2\text{O}$ ($v/v = 1/1$) was loaded in the micropipette to dissolve the residual Phen with the assistance of ultrasonic for 30 s (Fig. S3d in Supporting information), followed by nano-ESI MS analysis using the micropipette as the nano-ESI emitter. As shown in Fig. 2f, an obvious signal of $[\text{Phen} + \text{H}]^+$ was observed and the intensity was comparable to that in Fig. 2d with > 90% recovery. These results demonstrated that ER-nano-ESI MS was also an efficient method for analyzing organic analyte in strong acidic solution with rapidness (<2 min/sample) and accuracy (>90%). Besides, glutamine and arginine were further analyzed in the same way, and the results (Fig. S4 in Supporting information) were similar to those of Phen.

In addition, ER-nano-ESI MS continued its strong performance in the analysis of organic and metal analytes in hydrochloric acid (Fig. S5 in Supporting information).

To investigate the sensitivity of the ER-nano-ESI MS, Phen and Cu^{2+} were selected as representatives of organic compounds and metal ions, respectively. Different concentrations (1 μg/L, 10 μg/L, 50 μg/L, 100 μg/L, 200 μg/L, 500 μg/L, and 1000 μg/L) of Cu^{2+} and Phen in 0.1 mol/L HNO_3 were prepared and analyzed by ER-nano-ESI MS as mentioned above. Fig. 3a showed the standard curve between the intensity of $[^{63}\text{Cu} + 2(\text{Phen})]^{2+} + [^{63}\text{Cu} + 3(\text{Phen})]^{2+}$ and the concentration of Cu^{2+} . Fig. 3b showed the standard curve between the intensity of $[\text{Phen} + \text{H}]^+$ and the concentration of Phen. The limits of detection (LOD) of Cu^{2+} and Phen were 0.2 μg/L and 0.4 μg/L according to the formula $\text{LOD} = 3\sigma/a$, where “ σ ” is the standard deviation of blank solution ($n = 5$) and the “ a ” is the slope of standard curve.

To verify the application effect of this method on practical samples, several scenarios involved strong acidic solution were taken into account. A typical sample that easily comes to mind is the gastric juice, which is an important biological sample and can provide valuable clinicopathologic information on the molecular level for gastric disease without the diagnostic limitations of routine en-

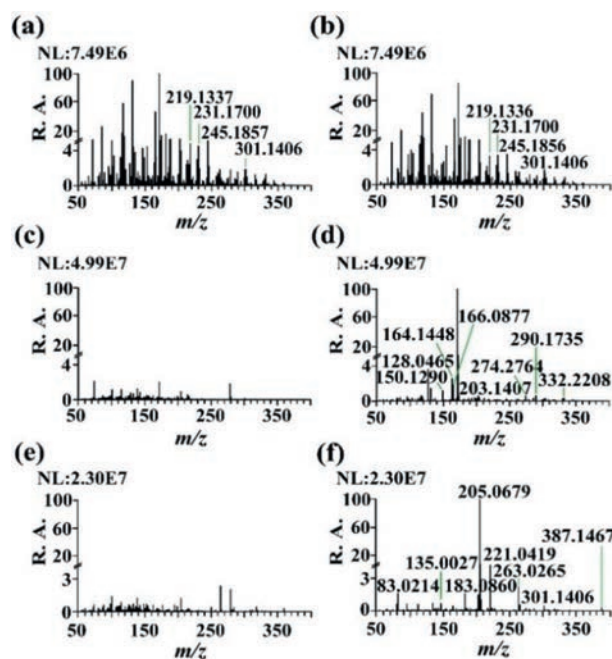


Fig. 4. Analysis of gastric juice by nano-ESI MS and ER-nano-ESI MS. Mass spectrum of gastric juice from gastric perforation patient by (a) nano-ESI MS and (b) ER-nano-ESI MS. Mass spectrum of gastric juice from pancreatic injury patient by (c) nano-ESI MS and (d) ER-nano-ESI MS. Mass spectrum of gastric juice from intestinal obstruction patient by (e) nano-ESI MS and (f) ER-nano-ESI MS. R. A. is the abbreviation of relative abundance.

doscopic practice [1]. It would be an important supplement to endoscopic images if the molecular information of gastric juice can be obtained in the meantime. Therefore, as a concept application, ER-nano-ESI MS was utilized for the rapid analysis of gastric juice, dispensing with complex sample pretreatment of traditional mass spectrometry.

Three kinds of gastric juice samples were collected from a gastric perforation patient (Sample-1), a pancreatic injury patient (Sample-2), and an intestinal obstruction patient (Sample-3), which were provided by The First Affiliated Hospital of Nanchang University. The pH values were tested to be about 6, 1, and 1 for Sample-1, Sample-2 and Sample-3, respectively. The solid residue in the gastric juice was removed by centrifugation at 10000 r/min prior to MS analysis. As shown in Figs. 4a and b, the mass spectrum obtained by nano-ESI MS (Fig. 4a) was almost the same as that obtained by ER-nano-ESI MS (Fig. 4b) for Sample-1 (pH 6), which indicated that ER-nano-ESI MS had identical performance with nano-ESI MS when analyzing the neutral or faintly acidic solution. However, for Sample-2 (pH 1) and Sample-3 (pH 1), the MS signals obtained by nano-ESI MS were very weak (Figs. 4c and e), while obvious MS signals were obtained by ER-nano-ESI MS (Figs. 4d and f), which further confirmed that the ER-nano-ESI MS could be a useful method for analysis of the strong acidic solution. Accurate m/z and the tandem MS results (Figs. S6-S8 in Supporting information) coupled with a library search (Human Metabolome Database, <https://hmdb.ca/>) were used to identify the metabolites. Table S1 (Supporting information) displayed the 14 identified metabolites in different gastric juice samples, such as $[\text{Leucyl-leucine} + \text{H}]^+$ (m/z 245.1856) and $[\text{Myriganon B} + \text{H}]^+$ (m/z 301.1406) in Sample-1, $[\text{Amino leucine} + \text{NH}_4]^+$ (m/z 164.1448) and $[\text{Leucyl-alanine} + \text{H}]^+$ (m/z 203.1407) in Sample-2, $[2,3\text{-Dihydroxy-2,4-cyclopentadien-1-one} + \text{Na}]^+$ (m/z 135.0027) and $[\text{L-Lysine hydrochloride} + \text{H}]^+$ (m/z 183.0860) in Sample-3, where most of the metabolites came from the food or environment. This study was approved by The First Affiliated Hospital of Nanchang University,

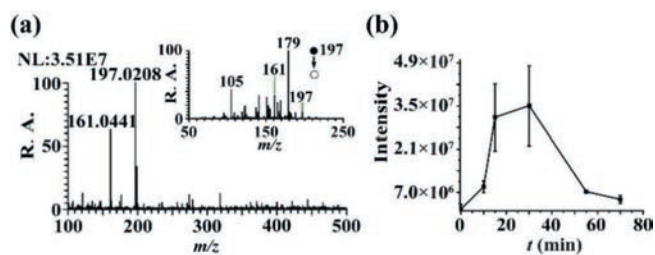


Fig. 5. Monitoring of the hydrochloric acid-catalyzed hydrolysis of cellulose by ER-nano-ESI MS. (a) The mass spectrum of the solution after reaction for 30 min. Inset is the tandem mass spectrum of m/z 197. (b) Signal intensity of m/z 197.0208 vs. reaction time. R. A. is the abbreviation of relative abundance. The error bar represents the standard deviation of three replicates.

and was performed in accordance with the local laws, regulations and regional ethic. All the experiments have passed the assessment of the Ethics Committee in the Nanchang University. All volunteers gave their informed consent.

Another common situation in which ER-nano-ESI MS can be useful is chemical reaction catalyzed by strong acid. Real-time analysis of compounds in reaction can dynamically monitor the reaction progress, which helps in understanding the reaction mechanism. ER-nano-ESI MS takes the advantages of rapidness (2 min/sample), high sensitivity, and nanoliter sample consumption, which enables fast and sensitive monitoring of the reaction process without disturbing the reaction. Herein, as a concept application, ER-nano-ESI MS was used to monitor the hydrolysis of cellulose.

10 g cellulose was added into 200 mL of 10% HCl solution, followed by heating up to 95 °C. Fig. 5a showed the MS results of the solution after reaction for 30 min. An obvious signal of m/z 197.0208 was observed accompanied by an apparent isotope peak $[M+2]^+$ with about 33% relative abundance, indicating that a chlorine element was included. Through a combination of the m/z and isotope peak, the signal of m/z 197.0208 could be attributed to $[C_6H_9O_5Cl+H]^+$. The obvious peak of m/z 161.0441 could be attributed to $[C_6H_8O_5+H]^+$. The inset of Fig. 5a displayed the CID result of m/z 197. An obvious peak of m/z 179 was obtained, which was the fragment ion generated by the loss of H_2O from m/z 197. The peak m/z 161 was also observed in the inset due to the loss of HCl from m/z 197. To further confirm the analytical results, 1 mg/L glucose in 1 mol/L HCl was also analyzed by ER-nano-ESI MS. The spectrum was displayed in Fig. S9 (Supporting information), of which the main peaks of m/z 161.0441 and m/z 197.0208 were the same as those in Fig. 5a. But when 1 mg/L cellulose in 1 mol/L HCl was analyzed as well, the peaks of m/z 161.0441 and m/z 197.0208 in the mass spectrum were ignorable. These results proved that the identification of m/z 161.0441 and m/z 197.0208 was correct. Thus, the peak of m/z 197.0208 was used as a quantitative ion to monitor the reaction process. Fig. 5b displayed the variation in signal intensity of m/z 197.0208 vs. reaction time. The concentration of glucose increased with the reaction progress and reached a peak value after 30 min. Then the concentration of glucose began to decrease, because the produced glucose would be further degraded into other by-products. This variation tendency was consistent with that reported in literatures [29]. These results demonstrate the ER-nano-ESI MS is a powerful method for monitoring the strong acid-catalyzed reaction.

In addition, strong acids, such as HCl and HNO_3 , were always used to extract the chemical composition of ores, where ER-nano-ESI MS would be helpful. Currently, with the improvement of ore analysis requirements, micro-area analysis has become an increasingly important method for studying the structure of ores by providing high-resolution information of the concentration and

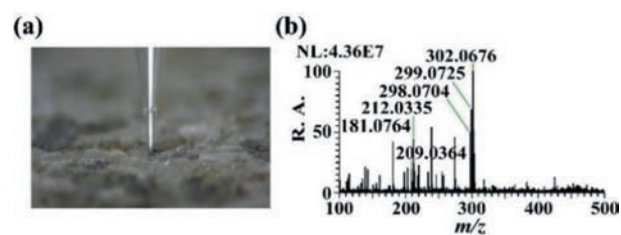


Fig. 6. Application of ER-nano-ESI MS for micro-area analysis of gabbro sample. (a) Microphotograph of the micro-area sampling. (b) Mass spectrum of the extraction of gabbro sample obtained by ER-nano-ESI MS. R. A. is the abbreviation of relative abundance.

distribution of elements. Although Laser ablation-inductively coupled plasma-mass spectrometry (LA-ICP-MS) [30] is widely used in micro-area analysis and takes the advantages of high spatial resolution, high sensitivity, and high speed of analysis, acids extraction can realize the extraction of various speciation by varying the extraction solution [31]. Herein, a concept application of the ER-nano-ESI MS for micro-area analysis of a thin section of gabbro was carried out.

A homemade device [28] was used for micro-area sampling, which could avoid the breakage of the micropipette tip. 1 nL of 1 mol/L HNO_3 was first loaded in the micropipette (the tip is 10 μm in diameter) by a microinjector. Then, the micropipette was accurately moved to the sample surface by a micromanipulator with the assistance of a microscope. Once the micropipette touched the sample (Fig. 6a), HNO_3 reacted with the minerals to extract the components. After extraction for 120 s, the extracted compounds were analyzed by ER-nano-ESI MS using 10 mg/L Phen (CH_3OH/H_2O , $v/v=1/1$) as a chelating agent, and the results were displayed in Fig. 6b. Compared with the mass spectrum of blank sample (Fig. S10 in Supporting information), obvious signals of $[Ni+2(Phen)]^{2+}$ (m/z 209.0364), $[Zn+2(Phen)]^{2+}$ (m/z 212.0335), $[Fe+3(Phen)]^{2+}$ (m/z 298.0704), $[Ni+3(Phen)]^{2+}$ (m/z 299.0725), $[Zn+3(Phen)]^{2+}$ (m/z 302.0676) were observed in Fig. 6b, which were all common elements in gabbro [32]. Moreover, the concentration of the extracted metal components in the micropipette can be calculated by the positive correlation relationship between signal intensity and concentration, which can provide the proportion or semi-quantitative results of the co-existing metal components [28]. These results demonstrate that the ER-nano-ESI MS is a promising method for micro-area analysis of ores, which will have great potential application in geology.

In summary, a method named ER-nano-ESI MS was developed for the analysis of strong acidic solutions, which involved three critical steps, namely "Evaporation", "Redissolution" and "nano-ESI MS". This method takes the advantages of high speed (<2 min/sample), low sample consumption (≤ 1 nL), high sensitivity (LOD = 0.2 $\mu g/L$), and high recovery (>90%). Proof-of-concept applications in the analysis of gastric juice (pH of the sample = 1), monitoring of the reaction catalyzed by strong acid (pH of the system = 0), and micro-area analysis of ore with a high spatial resolution (pH of the extraction solvent = 1) demonstrated the great application potential of present method in multiple fields.

Declaration of competing interest

The authors declare that they have no known competing financial interests or personal relationships that could have appeared to influence the work reported in this paper.

Acknowledgments

This work was supported by the National Natural Science Foundation of China (Nos. 21864001, 21727812 and 21765001), and the Ph.D. Start-up Foundation of East China University of Technology (No. DHBK2020001).

Supplementary materials

Supplementary material associated with this article can be found, in the online version, at doi:10.1016/j.ccl.2023.108578.

References

- [1] A. Tucci, M. Bisceglia, M. Rugge, et al., *Gastrointest. Endosc.* 66 (2007) 881–890.
- [2] A. Agrawal, K.K. Sahu, J. *Hazard. Mater.* 171 (2009) 61–75.
- [3] U. Kesime, A. Chrysanthou, M. Catulli, C.Y. Cheng, *J. Chem. Technol. Biot.* 93 (2018) 3374–3385.
- [4] Q.Y. Shao, B.L. Jiang, S. Huang, *Mater. Res. Express* 6 (2019) 0865b4.
- [5] W.X. Lv, X. Wang, J.H. Wu, H.Y. Li, F. Li, *Chin. Chem. Lett.* 30 (2019) 1635–1638.
- [6] W. Detpisuttitham, C. Phanthong, S. Ngamchana, P. Rijiravanich, W. Surareungchai, *J. Anal. Test.* 4 (2020) 291–297.
- [7] E. Laher, A. Zullo, C. Hassan, et al., *Helicobacter* 19 (2014) 417–424.
- [8] C. Spada, S. Piccirelli, *Methods Mol. Biol.* 2283 (2021) 21–27.
- [9] Y.A. An, S. Liu, Y.L. Wang, H.R. Tang, *Chin. Chem. Lett.* 31 (2020) 1827–1830.
- [10] H. Qi, L.Y. Jiang, Q. Jia, *Chin. Chem. Lett.* 32 (2021) 2629–2636.
- [11] M.D. Machado, E.V. Soares, H.M.V.M. Soares, *Environ. Sci. Pollut. Res.* 18 (2011) 1279–1285.
- [12] F. Wang, M.S. Guo, K. Wang, et al., *Rock Min. Anal.* 25 (2006) 263–269.
- [13] M.B. Revuelta, *Mineral Resources from Exploration to Sustainability Assessment*, Springer International Publishing AG, Switzerland, 2018.
- [14] M.Y. Anzabi, H. Yazdani, A. Bazgir, *Catal. Lett.* 149 (2019) 1934–1940.
- [15] K. Neubauer, E. Pruszkowski, *Spectroscopy* 32 (2017) 17–26.
- [16] G.D. Cao, Z.B. Song, Z.Y. Yang, et al., *Chin. Chem. Lett.* 32 (2021) 3207–3210.
- [17] P.S. Sreeja, K. Arunachalam, S. Saikumar, et al., *Biomed. Pharmacother.* 97 (2018) 1109–1118.
- [18] W. Lee, J. Um, K. Ko, et al., *J. Anal. Sci. Technol.* 11 (2020) 19.
- [19] C.W. Lee, H. Su, Y.D. Cai, et al., *Mass Spectrom.* 6 (2017) S0056.
- [20] C.W. Lee, H. Su, R.H. Lee, et al., *Clin. Chim. Acta* 485 (2018) 288–297.
- [21] H. Su, Y.P. Lin, S.C. Yang, et al., *Anal. Chim. Acta* 1066 (2019) 69–78.
- [22] P. Novak, T. Zuliani, R. Milacic, J. Scancar, *Anal. Chim. Acta* 915 (2016) 27–35.
- [23] M. Czaplicka, K. Jaworek, J. Klyta, *Desalin. Water Treat.* 172 (2019) 386–394.
- [24] F. Jiao, W. Li, K. Xue, C.R. Yang, W.Q. Qin, *Sep. Purif. Technol.* 227 (2019) 115705.
- [25] L.C. Zhao, J.G. Wang, X. Li, et al., *Chin. J. Anal. Chem.* 46 (2018) E1801–E1809.
- [26] J.A. Pienaar, A. Singh, T.G. Barnard, *Microb. Pathogenesis* 144 (2020) 104180.
- [27] H.N. Xu, L.G. Jin, Y. Cheng, *Sci. Adv. Mater.* 12 (2020) 1078–1089.
- [28] J.Q. Xu, D.C. Zhong, K. Chinglin, L.L. Song, H.W. Chen, *Anal. Chem.* 91 (2019) 8304–8309.
- [29] W.H. Chen, B.L. Pen, C.T. Yu, W.S. Hwang, *Bioresource Technol.* 102 (2011) 2916–2924.
- [30] B. Hattendorf, C. Latkoczy, D. Günther, *Anal. Chem.* 75 (2003) 341A–347A.
- [31] J.Q. Xu, F.L. Li, F. Xia, et al., *Sci. China Chem.* 64 (2021) 642–649.
- [32] V.A. Kreneva, E.N. Pechenkina, S.V. Fomichev, *Russ. J. Inorg. Chem.* 66 (2021) 253–257.